Stability of glued and embedded Glass Panes: Dunkerley straight Line as a conservative Estimate of superimposed buckling Coefficients

A. Arnold, L. Neumann, W. Hochhauser

Most recent ASC Reports

ASC
TU WIEN

Stability of glued and embedded Glass Panes: Dunkerley straight Line as a conservative Estimate of superimposed buckling Coefficients [⋆]

Anton Arnold [∗] **Lukas Neumann** [∗∗] **Werner Hochhauser** [∗∗∗]

[∗] *Institute for Analysis and Scientific Computing, Vienna University of Technology, A-1040 Wien, Austria (e-mail: anton.arnold@tuwien.ac.at),*
[∗∗] *Institute for Mathematics, Innsbruck University, A-6020 Innsbruck, Austria (e-mail: lukas.neumann@uibk.ac.at),*
[∗∗∗] *Institute of Architectural Sciences, Department of Structural Design and Timber Engineering, Vienna University of Technology, A-1040 Wien, Austria (e-mail: hochhauser@iti.tuwien.ac.at).*

Abstract:
We consider a rectangular glass pane as part of a stiffening and force-transmitting timber-glass composite building element. The glass pane is assumed to be both glued circumferentially and embedded into a timber substructure via block setting which enables a load transfer of horizontal forces via vitreous shear areas and compression diagonals within the glass. To verify the stability of the glass pane, the buckling coefficient has to be determined.
In this note we first present a PDE model (based on linear elasticity) for the stress tensor within the glass pane and the eigenvalue problem for buckling of the pane. These two equations (in weak formulation) are then solved subsequently with the software COMSOL, i.e. the computed stress field is an input coefficient for the eigenvalue problem of the plate equation. We are interested in the critical load that implies buckling. It is determined by zero becoming an eigenvalue of the plate equation. Numerical results are presented for pane geometries between 1:1 and 4:1. We also find that an additional transversal surface pressure does not influence the critical buckling loads (at linear order).
The maximum load is a non-linear function of the compression and shear forces applied at the boundary of the pane. To provide a simplified analysis for the practitioner, we prove that the Dunkerley straight line represents a conservative estimate for superimposed buckling coefficients and therefore for the critical buckling load. This mathematically rigorous proof is based on an application of the generalized Dunkerley theorem for eigenvalue problems.

Keywords: plate buckling, stability analysis, von Kármán plate equations, eigenvalue problem, FEM simulation, Dunkerley straight line

---

1. INTRODUCTION

The contribution of glass areas to the stiffness of a building has traditionally been neglected in design. And, so far, glass has been mainly a filling building material. It has rightfully been so because normal designs used for windows, e.g., provide relatively little strength and stability. In fact, the general assumption for such components has instead been that they should not be a part of the load bearing structure. However, fixed "windows" could offer a considerable contribution to the resistance of a building during horizontal loading if the following conditions are satisfied: properly designed glass panes that are structurally bonded to the frame; an adequate material selection; proper design principles for the practicing engineer; sufficiently stiff but yet ductile connections between the glass and the timber-frame that assure a ductile failure in the connection instead of a brittle failure of glass.

Wall components bear vertical loads like dead load, live loads, snow loads and in addition ensure the lateral stability in case of wind and earthquake loads. If large parts of walls or even entire walls are replaced by a glass facade, vertical loads can be transferred by beam and column systems but the lateral stiffening component is missing. In the case of horizontal loads, eliminating the stiffening component of an entire side of the building results in an unfavorable eccentricity, which also causes additional torsion stress on the residual wall panels. To avoid such statical problems it is necessary to utilize stiffening glass elements.

Lightweight building structures can nowadays be stiffened efficiently by means of glued and embedded timber-glass

composite panes. A novel construction principle enables load transfer of horizontal forces via vitreous shear areas and compression diagonals within the glass. Hence, conventional stiffening methods such as wind bracing become dispensable, Hochhauser (2011).

In this paper we shall analyze the stability of the stiffening glass pane. This is one of the most important proofs within the sizing of stiffening timber-glass composite panes, and it presupposes the identification of the glass panes buckling coefficient. In Fig. 1 we illustrate the boundary forces on the glass pane. Due to the superposition of two bearing mechanisms (block setting and glueing) within one pane, the buckling coefficients – amongst others depending on the way of load application – have to be superimposed too. But while the stress tensor within the pane is a linear combination of the two applied forces, the buckling coefficient and therefore the buckling load is *not a linear function* of the critical compression force and the critical shear force. Hence, the related eigenvalue problem for the pane buckling has to be solved numerically for each pair of applied forces. To simplify the situation in real applications, the superimposed buckling coefficient can be approximated by the Dunkerley straight line, which is a linear interpolation between the coefficients of the critical compression force and the critical shear force.

In this note we first present a numerical study of the accuracy of this approximation. Then we give a mathematical proof that the Dunkerley straight line represents a conservative estimate for the buckling coefficients in the present problem. So far, this fact was assumed to be known and "obvious", but a rigorous justification was missing.

The compression and shear forces acting on the glass pane give the considered system the structure of a *bifurcation problem:* Below the critical load the glass pane stays flat. In this paper we extend our work from Neumann et al. (2011) by also including a uniform surface load on the glass pane which might be caused by wind forces or isochoric pressure within insulated glass. With respect to this third force, the considered system is of a different nature: The glass bends as a *continuous response* to this force (this distinction is also discussed in §3.4.1.5 of Englhardt (2007)).

2. MATHEMATICAL MODEL

The (isotropic) glass pane occupies the domain $\Omega := (0, a) \times (0, b)$. On this domain the transversal pane deflection $u(x, y)$ and the Airy stress function $F(x, y)$ satisfy the von Kármán plate equations, see Timoshenko et al. (1961); Altenbach et al. (1998):

$$\Delta^2 u = \frac{1}{D}\left[p + \frac{\partial^2 F}{\partial y^2}\partial_x^2 u - 2\frac{\partial^2 F}{\partial x \partial y}\partial_x \partial_y u + \frac{\partial^2 F}{\partial x^2}\partial_y^2 u \right], \ (1)$$

$$\Delta^2 F = Eh\left[\left(\frac{\partial^2 u}{\partial x \partial y} \right)^2 - \frac{\partial^2 u}{\partial x^2}\frac{\partial^2 u}{\partial y^2} \right]. \quad (2)$$

Here, p denotes the (uniform) surface pressure. And $D = \frac{Eh^3}{12(1-\nu^2)}$ is the stiffness of the pane, with E the modulus of elasticity and ν Poisson's ratio. h, the thickness of the pane does not appear in (1), since we normalized the stress components by it. I.e., we assume that the boundary stresses are given as force/length.
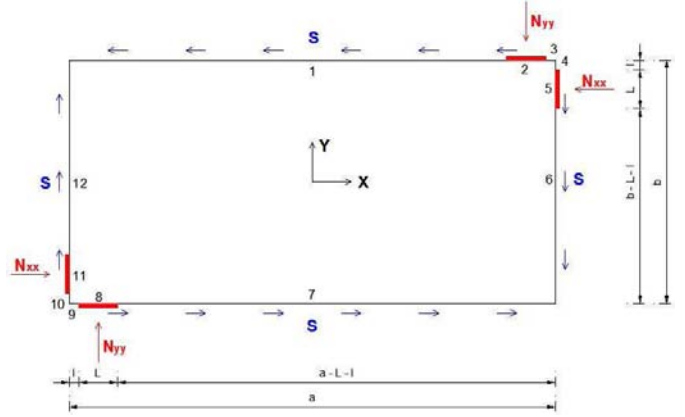

Fig. 1. Illustration of the tested pane geometry. A constant shear force of strength S is applied on all edges. Compression forces (of strength N_{xx} and N_{yy}) are applied at the four block settings of length L, which are located at the distance $l > 0$ from the corners. The compression forces are in balance and exert no torque on the pane.

In this paper we shall only consider small pressures p such that the (pre-buckling) deflections of the pane are small w.r.t. its thickness. In this case the nonlinear terms in (2) can be neglected (cf. Altenbach et al. (1998)) and it simplifies to

$$\Delta^2 F = 0. \quad (3)$$

Hence, (1), (3) decouple into two linear equations that have to be solved consecutively. In the absence of a surface load (i.e. for $p = 0$) this is in fact no approximation, since the pane stays flat in the pre-buckling regime.

We assume the glass pane to be simply supported on all four edges. Hence, the boundary conditions for (1) read $u = \Delta u = 0$ on $\partial\Omega$. To formulate the boundary conditions for (3) we first have to relate the Airy stress function F to the stress tensor in the pane:

$$\boldsymbol{\sigma}(x, y) = \begin{pmatrix} \sigma_x & \tau_{xy} \\ \tau_{xy} & \sigma_y \end{pmatrix} := \begin{pmatrix} \partial_y^2 F & -\partial_x \partial_y F \\ -\partial_x \partial_y F & \partial_x^2 F \end{pmatrix}. \quad (4)$$

The boundary conditions on $\boldsymbol{\sigma}$ read

$$\boldsymbol{\sigma} \cdot n = t, \quad (5)$$

where n denotes the exterior unit normal vector, and t the applied stress vector on $\partial\Omega$. It is composed of the pressure (of strength N_{xx} and N_{yy}) due to the block settings and a uniform shear force (of strength S) due to the glueing (cf. Fig. 1). In order to ensure balance of torque we require $N_{yy} = \gamma N_{xx}$ with $\gamma = \frac{b-2l-L}{a-2l-L}$.

For F we shall impose Dirichlet and Neumann boundary conditions: $F = f$, $\frac{\partial F}{\partial n} = g$ on $\partial\Omega$. And the boundary data f, g are obtained from $\boldsymbol{\sigma} \cdot n = t$ by integrating the boundary data σ_x, σ_z, τ_{xy} along $\partial\Omega$, using the relation (4). As a normalization we choose $F(0, 0) = F_x(0, 0) = F_y(0, 0) = 0$, e.g. But this ambiguity (an additive first order polynomial in x and y) again drops out in (1). The imposed balance of forces and torques implies C^1–compatibility of the boundary data F, ∇F when integrating along the closed curve $\partial\Omega$.

The coefficients of (1) are the components of the stress tensor (cf. (4)). From a numerical point of view it is inconvenient to obtain them from the fourth order equation (3). Instead they can be obtained more easily from the elliptic PDE system

$$\operatorname{div} \boldsymbol{\sigma} = 0 , \qquad \partial_y^2 \sigma_x + \partial_x^2 \sigma_y - 2 \partial_{xy} \tau_{xy} = 0 . \quad (6)$$

By linearity of the boundary conditions, the resulting stress tensor has the form

$$\boldsymbol{\sigma}(x,y) = N_{xx} \, \boldsymbol{\sigma}_N(x,y) + S \begin{pmatrix} 0 & -1 \\ -1 & 0 \end{pmatrix} , \qquad (7)$$

where $\boldsymbol{\sigma}_N$ is the stress tensor due to the pressures $N_{xx} = 1$, $N_{yy} = \gamma$ on the block settings only. Hence, we only have to compute $\boldsymbol{\sigma}_N$ numerically once, by using the FEM–software COMSOL. The obtained coefficients are then used as input for the linear plate equation with Navier bearing (i.e. with the boundary conditions $u = \Delta u = 0$ on $\partial\Omega$):

$$-\Delta^2 u + \frac{1}{D} \left(p + \sigma_x \partial_x^2 u + 2\tau_{xy} \partial_x \partial_y u + \sigma_y \partial_y^2 u \right) = \lambda \, u \quad \text{on } \Omega . \tag{8}$$

For $p = 0$ this is an eigenvalue problem, with $\lambda \in \mathbb{R}$. The main question is: For which pair of loads (i.e. pressure N_{xx} and shear force S) does the pane buckle? Buckling corresponds to $\lambda = 0$ becoming an eigenvalue of (8). The sign of λ was chosen such that $\lambda \geq 0$ corresponds to the formation of a buckle.

Numerically we actually solve its weak formulation for u in the Sobolev space $H^2(\Omega) \cap H_0^1(\Omega)$:

$$- \int_\Omega \Delta u \Delta v \, \mathrm{d}(x,y) - \frac{1}{D} \int_\Omega (\nabla u)^T \boldsymbol{\sigma} \nabla v \, \mathrm{d}(x,y) \tag{9}$$

$$= \lambda \int_\Omega uv \, \mathrm{d}(x,y) \qquad \forall v \in H^2(\Omega) \cap H_0^1(\Omega) .$$

The bilinear form on the l.h.s. of (9) is symmetric and bounded on $\left(H^2(\Omega) \cap H_0^1(\Omega) \right)^2$. Boundedness of the second term in (9) follows from $\boldsymbol{\sigma} \in L^2(\Omega)$ (cf. Lemma 1 below) and the Sobolev embedding $H^1(\Omega) \hookrightarrow L^q(\Omega)$ for all $1 \leq q < \infty$. Without lateral forces (i.e. $S = N_{xx} = 0$) the negative bilinear form is coercive, and hence all eigenvalues are negative. But for large enough external forces the largest eigenvalue becomes non-negative, and a buckle forms in the shape of the corresponding eigenfunction $u^0(x,y)$.

Next we consider (8) for $p \neq 0$ and with external compression and shear forces below the critical buckling load. Then the negative bilinear form from (9) is still coercive. Hence, the inhomogeneous equation (8) (with $\lambda = 0$) has a unique weak solution $u_p(x,y)$. It represents the bending of the pane under the applied surface pressure in the pre-buckling regime. But at the critical buckling load 0 becomes an eigenvalue for (9). Hence (8) has a non-unique solution (in fact $u_p + c \, u^0$ with $c \in \mathbb{R}$). And this indicates the buckling of the glass pane with surface pressure.

From this discussion we see that an applied surface pressure does *not* modify the critical buckling loads – under our assumption of small deflections and within the linear plate theory. In a future continuation of our work we plan to include higher order approximations of (2). This will allow us to analyze the expected higher order effect (presumably of the order p^2) of the transversal surface pressure
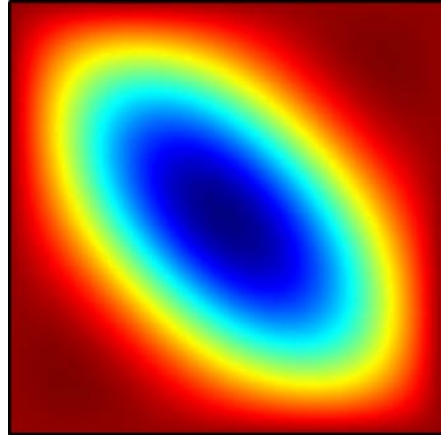

Fig. 2. Pure shear buckle at $S = S^{crit}$, $\lambda_0 \approx 0$; aspect ratio 1:1.

on the critical buckling loads. Theoretical approaches to this topic (based on series expansions) are referred to in §3.4.1.6 of Englhardt (2007).

3. NUMERICAL RESULTS

For the numerical solution of (6) we use the FEM–software COMSOL in the application mode "plain stress". As mentioned before, we only have to compute $\boldsymbol{\sigma}_N(x,y)$ once. Then the stress tensor $\boldsymbol{\sigma}(x,y)$ for general boundary loads is given by (7). It provides the coefficients for the eigenvalue problem (9) (in weak formulation). The critical buckling loads N_{xx}^{crit} and S^{crit} are determined by bisection: The applied load is varied until the maximum eigenvalue satisfies $\lambda = 0$. For more numerical and algorithmic details we refer to Neumann et al. (2011).

For our simulations we use the parameters $b = 1.25$m, $L = 20$cm, $l = 5$cm. We shall now present numerical results for the aspect ratios 1:1, 2:1, and 4:1, which implies $\gamma = 1$, 0.4318, 0.2021, resp. First we consider the situation of a pure shear stress. Here, the buckling coefficient is defined as $k_{shear} = \frac{S^{crit}b^2}{\pi^2 D}$, where S^{crit} is again related to the length of the edge. Our numerical simulations for the three geometries yield a buckling coefficient of $k_{shear} \approx 9.34$, 6.55, and 5.62, resp. This can be compared to the results from the theoretical approximation method (based on global Fourier polynomials on Ω) from Timoshenko et al. (1961): Their results give $k_{shear} \approx 9.34$, 6.60, 5.70, resp. The corresponding eigenfunctions for the geometries 1:1 and 4:1 are given in Fig. 2 and Fig. 3. The eigenfunction for the case 2:1 is given in Neumann et al. (2011).

Next we turn to the situation of a pure compression stress. The eigenfunctions corresponding to the critical compression load for the geometries 1:1 and 4:1 are given in Fig. 4 and Fig. 5, the case 2:1 is given in Neumann et al. (2011).

Finally we consider the superposition of shear and compression forces. Fig. 6 shows the interaction diagram for the combined buckles. The critical loads are obtained by numerically solving the eigenvalue problem (9) for appropriate pairs (N_{xx}, S). For a fixed choice of $0 < N_{xx} <$
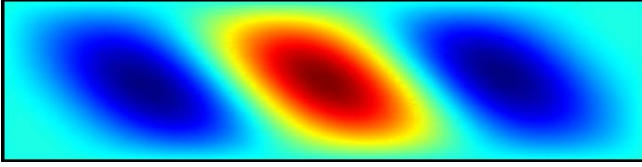
Fig. 3. Pure shear buckle at $S = S^{crit}$, $\lambda_0 \approx 0$; aspect ratio 4:1.
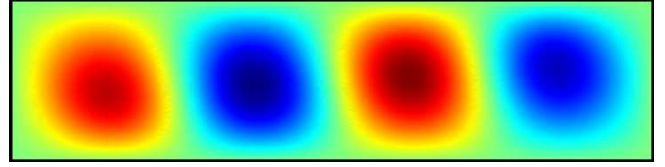

Fig. 5. Pure compression buckle at $N_{xx} = N_{xx}^{crit}$, $\lambda_0 \approx 0$; aspect ratio 4:1.
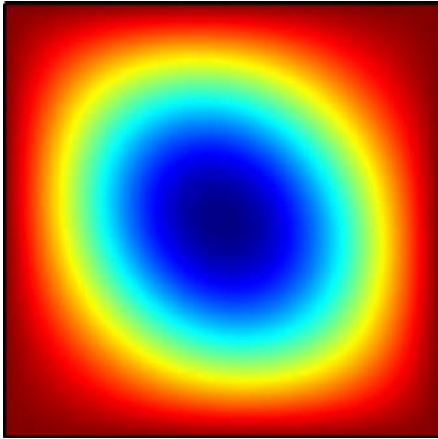

Fig. 4. Pure compression buckle at $N_{xx} = N_{xx}^{crit}$, $\lambda_0 \approx 0$; aspect ratio 1:1.

N_{xx}^{crit}, S is increased until 0 becomes an eigenvalue. The curved lines in Fig. 6 are the numerical results for our three geometries. They are compared to the linear interpolation between $(0, S^{crit})$ and $(N_{xx}^{crit}, 0)$ – the *Dunkerley straight line*.

We remark that a buckling analysis for a similar structure (simply supported plate under combined shear and longitudinal compression on two whole edges) was cited in §4.2.4 of Ziemian (2010). For aspect ratios $a/b \geq 1$ the interaction diagram there can be approximated quite well by a parabola.

4. DUNKERLEY STRAIGHT LINE

We shall now provide a simplified analysis of the buckling coefficient for the practitioner. In contrast to the multitude of simulations leading to the nonlinear result in Fig. 6, our subsequent approximation requires only to determine numerically the critical compressive force N_{xx}^{crit} (without shear) and the critical shear force S^{crit} (without compression), which both depend linearly on the corresponding
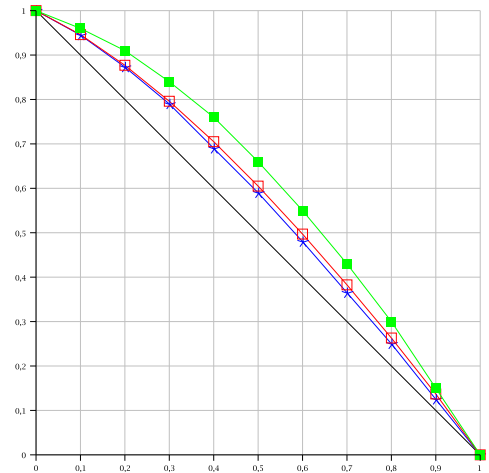

Fig. 6. Interaction diagram for superimposed shear and compression buckles for three aspect ratios of the glass pane: Dunkerley straight line (black solid line) and nonlinear, numerical results (blue stars 1:1, red open squares 2:1, green solid squares 4:1). Ordinate: ratio of shear S and critical shear S^{crit}. Abscissa: ratio of compressive force N_{xx} and critical compressive force N_{xx}^{crit}.

buckling coefficients. Then, the Dunkerley straight line represents a conservative estimate for the superimposed coefficients and therefore for the critical buckling load (S as a function of N_{xx}, cf. Fig. 6). Such an approximation result is taken for granted in many mechanical systems that lead to eigenvalue problems with a nonlinear superposition of subsystems. But a rigorous justification for the system considered here was missing.

Here we present a mathematically rigorous proof, which is based on an application of the generalized Dunkerley theorem for eigenvalue problems (cf. Th. 2-2 in Tarnai (1999), Th. 3.1 in Tarnai (1995)). The key step of the

proof is to show that the quadratic forms pertaining to the lower order terms in (8) are *completely continuous* (in the sense of §3.3, Weinberger (1974)) w.r.t. $\langle \Delta^2 u, u \rangle$. In order to guarantee the applicability of that theorem we first need a technical result:

Lemma 1. The solution of (6)-(5) satisfies $\boldsymbol{\sigma} \in L^2(\Omega)$.

<u>Proof:</u> The discontinuous boundary data of σ_x, σ_y do not lie in the Sobolev space $H^{\frac{1}{2}}(\partial\Omega)$. Hence, they cannot be extended to $H^1(\Omega)$–functions. And therefore the elliptic system (6)-(5) cannot be treated by the standard theory.

Thus we consider now the equivalent problem for the Airy stress function $F(x,y)$. As discussed in §2 it satisfies the biharmonic equation

$$\Delta^2 F = 0 \quad \text{in } \Omega; \qquad F = f, \ \frac{\partial F}{\partial n} = g \quad \text{on } \partial\Omega. \quad (10)$$

In our application the boundary stresses satisfy σ_x, σ_y, τ_{xy} $\in L^\infty(\partial\Omega)$. And this implies $f \in W^{2,\infty}(\partial\Omega) \subset H^{\frac{3}{2}}(\partial\Omega)$, $g \in W^{1,\infty}(\partial\Omega) \subset H^{\frac{1}{2}}(\partial\Omega)$. Moreover, σ_x, σ_y vanish identically on $\partial\Omega$ close to the corners. Therefore, there exists an $H^2(\Omega)$–extension F_0 with $F_0\big|_{\partial\Omega} = f$, $\frac{\partial F_0}{\partial n}\big|_{\partial\Omega} = g$. A standard, weak formulation of (10) then yields $\tilde{F} := F - F_0 \in H_0^2(\Omega)$, and $\boldsymbol{\sigma} \in L^2(\Omega)$ follows. $\square$

Remark 2. We point out that an $H^2(\Omega)$–extension of boundary data $f \in H^{\frac{3}{2}}(\partial\Omega)$, $g \in H^{\frac{1}{2}}(\partial\Omega)$ always exists for Ω convex with smooth boundary (cf. §IV.4.3 in Dautray et al. (2000), §2.7 in Brezzi et al. (1984)). But on polygonal boundaries the data has to satisfy two compatibility conditions at the corners (cf. Th. 1.5.2.4 in Grisvard (1985)): Continuity of f and a certain "integral compatibility" between the tangential derivative of f and g on the neighboring edge. This latter condition would be violated for $l = 0$ in our application. Therefore we require that the block settings are located at some distance from the corners. $\square$

Now we have the following lower bound for the critical buckling load $S = S(N_{xx})$:

Theorem 3. $S/S^{crit} \geq 1 - N_{xx}/N_{xx}^{crit}$ for $0 \leq N_{xx} \leq N_{xx}^{crit}$.

<u>Proof:</u> According to (7), the stress tensor $\boldsymbol{\sigma}$ depends linearly on N_{xx} and S. Hence, we first write the plate equation (8) with $p = 0$ as generalized eigenvalue problem:

$$(A - \lambda(B_1 + B_2))u = 0. \quad (11)$$

Here, the L^2–symmetric operators $A := \Delta^2 \geq 0$, $B_1 := -\frac{2\alpha}{D}S^{crit}\partial_x\partial_y$, $B_2 := \frac{(1-\alpha)}{D}N_{xx}^{crit}(\sigma_x\partial_x^2 + 2\tau_{xy}\partial_x\partial_y + \sigma_y\partial_y^2)$ are all defined on $\mathcal{D} = \{v \in H^4(\Omega) \,|\, v\big|_{\partial\Omega} = \Delta v\big|_{\partial\Omega} = 0\}$ (using $\boldsymbol{\sigma}_N \in L^2(\Omega)$ and the Sobolev embedding $H^2(\Omega) \hookrightarrow L^\infty(\Omega)$). The components of the stress tensor $\boldsymbol{\sigma}_N$ are denoted by σ_x, σ_y, τ_{xy} and $\alpha \in (0,1)$ is arbitrary. Our goal is to estimate the smallest positive eigenvalue λ.

<u>Step 1:</u> Using the Poincaré inequality yields

$$|\langle B_1 u, u \rangle| = \frac{2\alpha}{D}S^{crit}\left|\int_\Omega (\partial_x\partial_y u)\, u\, \mathrm{d}(x,y)\right| \leq C\langle Au, u\rangle$$
$$\forall u \in \mathcal{D}, \ (12)$$

and analogously for B_2.

<u>Step 2:</u> Here we shall show that the quadratic functionals $\langle B_j u, u \rangle$ ($j = 1, 2$) are completely continuous w.r.t. $\langle Au, u \rangle$. Following the definition in §3.3, Weinberger (1974) we hence have to show that the constant C in (12) can be chosen arbitrarily small, provided that $l_i(u) = 0$ for a finite set of (still to be chosen) linear functionals l_i, $1 \leq i \leq k$ on $L^2(\Omega)$.

$u \in L^2(\Omega)$ has the Fourier representation

$$u(x,y) = \sum_{m,n\in\mathbb{Z}} u_{mn}\, \varphi_{mn}(x,y), \quad (13)$$

with

$$\varphi_{mn} = \frac{1}{ab}e^{\frac{2\pi imx}{a}}\, e^{\frac{2\pi iny}{b}}.$$

Now we choose $\epsilon = \frac{ab}{\pi^2 MN}$ and we assume that $u_{mn} = 0$ holds, if $|m| < M$ and $|n| < N$. This implies

$$|\langle \partial_x\partial_y u, u \rangle| \leq \frac{1}{ab}\sum_{m,n}\frac{2\pi|m|}{a}\frac{2\pi|n|}{b}|u_{mn}|^2$$
$$\leq \frac{\epsilon}{a^2 b^2}\sum_{m,n}\frac{32\pi^4 m^2 n^2}{a^2 b^2}|u_{mn}|^2$$
$$\leq \epsilon\langle \Delta^2 u, u\rangle,$$

and the complete continuity of $\langle B_1 u, u \rangle$ w.r.t. $\langle Au, u \rangle$ follows. Here, we chose the finitely many functionals $l_{mn}(u) := \langle u, \varphi_{mn} \rangle$ with $m < M$ and $n < N$.

For B_2 we shall only consider the term $\sigma_x\partial_x^2$, since the remaining two terms can be analyzed analogously. For the case $u_{mn} = 0$ (if $|m| < M$ and $|n| < N$) the representation (13) and Hölder's inequality imply:

$$ab\|u\|_{L^\infty(\Omega)} \leq \sum_{m,n}|u_{mn}|$$
$$\leq \left\|(m^2 + n^2)u_{mn}\right\|_{\ell^2(\mathbb{Z}^2)}\left\|\frac{1}{m^2+n^2}\right\|_{\ell^2(\{u_{mn}\neq 0\})}$$
$$= \|\Delta u\|_{L^2(\Omega)}\,\epsilon_{MN},$$

where $\epsilon_{MN} = \mathcal{O}(\frac{1}{M+N})$. This estimate and the Hölder inequality yield

$$|\langle \sigma_x\partial_x^2 u, u \rangle| \leq \|\sigma_x\|_{L^2(\Omega)}\|\partial_x^2 u\|_{L^2(\Omega)}\|u\|_{L^\infty(\Omega)}$$
$$\leq \|\sigma_x\|_{L^2(\Omega)}\|\Delta u\|_{L^2(\Omega)}^2\frac{\epsilon_{MN}}{ab}.$$

Now the result follows with the same functionals as before.

<u>Step 3:</u> So far we have verified the assumptions for using the generalized Dunkerley–Theorem. Since the operator A is strictly positive, (12) also implies $A - \lambda_1 B_1 > 0$ for $|\lambda_1|$ small enough. The definition of S^{crit} clearly shows that $\lambda_1 = 1/\alpha$ is the smallest positive eigenvalue. Analogously, the definition of N_{xx}^{crit} implies that $\lambda_2 = 1/(1-\alpha)$ is the smallest positive eigenvalue of $A - \lambda_2 B_2 = 0$. Now the Dunkerley–Theorem yields the estimate $1/\lambda \leq \alpha + (1-\alpha)$ for the smallest positive eigenvalue of (11). And hence $\lambda \geq 1$.

Thus we have proved that the pair of boundary forces $\left(\lambda(1-\alpha)N_{xx}^{crit}, \lambda\alpha S^{crit}\right)$ can only lead to a zero-eigenvalue in (8) (and hence the formation of a buckle) if $\lambda \geq 1$

holds. $\lambda \geq 1$ means that this point on the critical buckling curve $S(N_{xx})$ lies "above" the Dunkerley straight line, $\left\{((1-\alpha)N_{xx}^{crit}, \alpha S^{crit}) \,|\, \alpha \in [0,1]\right\}$, cf. Fig. 6. □

5. CONCLUSION

Timber-glass hybrid elements meet modern architecture's demands and can help increase the use of timber as building material as well as the statical use of glass panes and plates. Timber-glass composites have a lot of potential to be discovered.

In this paper one of the most important proofs within the sizing of stiffening timber-glass composite panes, the proof of stability of glass panes, has been studied and therefore a basis for the simplified calculation of buckling coefficients via the Dunkerley straight line has been provided. Due to the fact, that numerically determined critical buckling loads are not that much higher than buckling loads calculated via the Dunkerley straight line, we suggest the use of the linear interaction for determination of buckling coefficients of glued and embedded timber-glass composite panes. If the critical buckling loads of both load cases are known, the Dunkerley straight line represents a lower bound for a combination of both compression diagonal and shear forces, while (exact) numerical calculations require lots of computational effort. This high effort only seems justifiable for extremely material optimized applications, independently of the width-to-height ratio from 1:1 to 4:1 of the glass pane. Furthermore, it has been shown that additional uniform surface loads due to wind forces or isochoric pressure within insulated glass do not affect the critical buckling load of stiffening glass panes, provided that linear and small-deformation theories are valid.

All things considered, the Dunkerley straight line represents an adequate and simple calculation method for the critical buckling load of stiffening timber-glass composite panes even if additional transversal loads have to be expected. Analyzing nonlinear, higher order effects of transversal loads will be the topic of a subsequent work.

REFERENCES

Altenbach, H., Altenbach, J., and Naumenko, K.: *Ebene Flächentragwerke: Grundlagen der Modellierung und Berechnung von Scheiben und Platten*, Springer, Berlin-Heidelberg, 1998.

Brezzi, F., and Gilardi, G.: *Fundamentals of P.D.E. for numerical analysis*, preprint n. 446 of Istituto di Analisi Numerica, Pavia, (1984).

Dautray, R., and Lions J.-L.: *Mathematical Analysis and Numerical Methods for Science and Technology - vol 2. Functional and Variational Methods*. Springer-Verlag, Berlin-Heidelberg-New York (2000).

Englhardt, O.: *Flächentragwerke aus Glas - Tragverhalten und Stabilität*, PhD-thesis: University of Natural Resources and Life Sciences, Vienna 2007.

Grisvard, P.: *Elliptic Problems in Nonsmooth Domains*. Pitman Publishing Inc., 1985.

Hochhauser, W.: *Ein Beitrag zur Berechnung und Bemessung von geklebten und geklotzten Holz-Glas-Verbundscheiben*, PhD-thesis: Vienna University of Technology, 2011.

Neumann, L., Arnold, A., and Hochhauser, W.: *Zur Stabilität von geklebten und geklotzten Glasscheiben: Beurteilung der Dunkerley'schen Geraden zur Beulwertbestimmung*, submitted 2011.

Tarnai, T.: *Summation theorems concerning critical loads of bifurcation*, pp. 23–58 in *Structural Stability in Engineering Practice* (L. Kollár ed.), Taylor & Francis, London, 1999.

Tarnai, T.: *The Southwell and the Dunkerley theorems*, pp. 141–185 in *Summation theorems Structural Stability* (T. Tarnai ed.), CISM Courses and Lecture No. 354, Springer, Wien, 1995.

Timoshenko, S.P., and Gere, J.M.: *Theory of elastic stability*, 2nd edition, McGraw-Hill, 1961.

Weinberger, H.F.: *Variational Methods for Eigenvalue Approximation*, CBMS-NSF Reg. Conf. Ser. in Appl. Math. No. 15, SIAM, Philadelphia, 1974.

Ziemian, R.D. (Ed.): *Guide to Stability Design Criteria for Metal Structures*, John Wiley & Sons, Hoboken, USA, 2010.